Tuning the Hole Injection Barrier at the Organic/Metal Interface with Self-Assembled Functionalized Aromatic Thiols

Wei Chen,[†] Chun Huang,[‡] Xing Yu Gao,[†] Li Wang,[†] Chang Gua Zhen,[‡] Dongchen Qi,[†] Shi Chen,[†] Hong Liang Zhang,[†] Kian Ping Loh,[§] Zhi Kuan Chen,*[,‡] and Andrew Thye Shen Wee*[,†]

Department of Physics, National University of Singapore, 2 Science Drive 3, Singapore 117542, Singapore, Institute of Materials Research and Engineering, 3 Research Link, Singapore 117602, Singapore, and Department of Chemistry, National University of Singapore, 3 Science Drive 3, Singapore 117543, Singapore

Received: September 7, 2006; In Final Form: October 13, 2006

Self-assembled functionalized aromatic thiols (oligophenylenes composed of building blocks of dimethoxy-substituted phenylenes, perfluoro-substituted phenylenes, and a terminal thiol group) were used to tune the hole injection barrier (Δ_h) of copper(II) phthalocyanine (CuPc) on Au(111). Synchrotron-based high-resolution photoemission spectroscopy study reveals a significant reduction of Δ_h by as much as 0.75 eV from $\Delta_h = 0.9$ eV for CuPc/Au(111) to $\Delta_h = 0.15$ eV for CuPc/BOF/Au(111), where BOF represents 4-pentafluorophenyl-1-(*p*-thiophenyl)-2,5-dimethoxybenzene. The delocalized π orbitals of these functionalized aromatic thiols greatly facilitate effective charge transfer (hole or electron) across the SAM interface as compared to alkanethiols, hence making this novel interface modification scheme a simple and effective way to tune the hole injection barrier. This method has potential applications in molecular electronics, organic light-emitting diodes (OLED), organic field-effect transistors (OFETs), and organic solar cells.

Introduction

Understanding and tuning the charge (hole or electron) injection barrier between electroactive conjugated molecule overlayers and metal, semiconductor, or conducting polymer substrates is critical to many technologically important applications, including organic light-emitting diodes (OLED), organic field-effect transistors (OFETs), organic solar cells, and molecular electronics.[1−6] A number of interface modification schemes have been developed to tune the charge injection barrier, especially the hole injection barrier (Δ_h), and hence to improve the device performance.[2−9] Recently, a dramatic lowering of Δ_h by as much as 1.2 eV has been achieved by inserting an electron acceptor layer of tetrafluoro-tetracyanoquinodimethane (F4-TCNQ) between the organic layers and Au substrate.[3a] There has been a burgeoning interest in modifying Δ_h by forming a self-assembled monolayer with different intrinsic dipole moments on metal or conductive transparent metal oxide substrate surfaces.[5,6,9−11] For example, self-assembled dipole molecules on indium tin oxide (ITO) substrates have been used to successfully improve hole injection in conjugated polymers, as well as charge collection in organic solar cells.[6] Hanson et al. have also demonstrated that very high current density in double-layer light-emitting devices can be achieved by forming a covalently bonded monolayer of π-conjugated organic semiconductor on ITO surfaces.[5b]

For most undoped organic/SAMs or organic/organic heterojunctions, the interface is dominated by a near vacuum level alignment due to the weak van der Waals intermolecular interaction between organic materials if there is no charge transfer at the interface.[1] It has been found that the vacuum level or work function of metal or ITO can be effectively modified by different dipolar SAMs.[5,6,9−11] Therefore, the general concept of tuning Δ_h between electroactive conjugated molecule overlayers and the underlying electrodes is to first tune the vacuum level of the electrodes over a wide range using dipolar SAMs, thereby achieving effective adjustment of the relative position (relative to the Fermi level of electrodes) of the highest occupied molecular orbital (HOMO) of the deposited organic molecules on the SAM-modified electrodes. In this paper, self-assembled functionalized aromatic thiols [BBB, 1-(*p*-thiophenyl)-4-phenylbenzene; BOO, 4-(*p*-thiophenyl)-2,2′,5,5′-tetramethoxy-biphenyl; BFO, 1-(*p*-thiophenyl)-4-(2′,5′-dimethoxyphenyl)-tetrafluorobenzene; BOF, 4-pentafluorophenyl-1-(*p*-thiophenyl)-2,5-dimethoxybenzene] were used to tune Δ_h between electroactive conjugated molecule overlayers and Au(111) substrate. The structures of the self-assembled monolayers (SAMs) are shown in Figure 1 by schematic drawings. Copper(II) phthalocyanine (CuPc), used widely in OFETs and organic solar cells, was chosen here as a model system to evaluate the effectiveness of tuning Δ_h with functionalized SAMs. With the use of synchrotron-based high-resolution photoemission spectroscopy (PES), a significant reduction of Δ_h by up to 0.75 eV was observed after deposition of 5 nm of CuPc on BOF/Au(111), relative to that of CuPc/Au(111) ($\Delta_h = 0.9$ eV).

Experimental Section

Synchrotron-Based High-Resolution Photoemission Spectroscopy (PES) and Near-Edge X-ray Absorption Fine Structure (NEXAFS) Measurements. The PES and NEXAFS experiments were carried out at the Surface, Interface and Nanostructure Science (SINS) beamline of the Singapore Synchrotron Light Source (SSLS).[12] The NEXAFS measure-

* Corresponding authors. Phone: 65-65166362 (A.T.S.W); 65-68744331 (Z.K.C.). Fax: 65-67776126 (A.T.S.W.); 65-68720785 (Z.K.C.). E-mail: phyweets@nus.edu.sg (A.T.S.W.); zk-chen@imre.a-star.edu.sg (Z.K.C.).
[†] Department of Physics, National University of Singapore.
[‡] Institute of Materials Research and Engineering.
[§] Department of Chemistry, National University of Singapore.

10.1021/jp065821q CCC: $33.50
Published on Web 11/23/2006

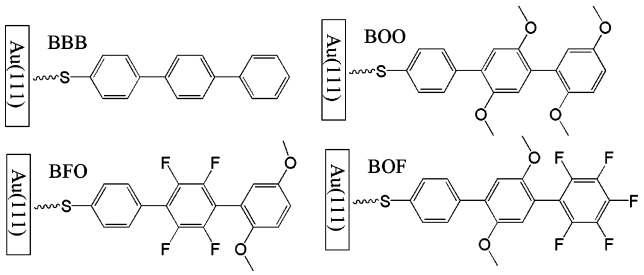

Figure 1. Schematic drawings of structures of BBB/Au(111), BOO/Au(111), BFO/Au(111), and BOF/Au(111).

ments were performed in total electron yield (TEY) mode with a photon energy resolution of 0.1 eV. The TEY signal, measured via the sample drain current, comprises all electrons escaping from the specimen as a result of the cascade process initiated by photon absorption.[13] The linear polarization factor of synchrotron light at the SINS beamline was measured to be about 0.95. The intensities of all the spectra were normalized to the total incoming photon flux measured with a gold grid. The photon energies were calibrated using the Fermi level (E_F) and Au $4f_{7/2}$ core level from an Ar sputter-cleaned poly gold reference sample, mounted close to the sample on the sample stage. The binding energies of all PES spectra were normalized to the Fermi level of the Au foil. The work functions (ϕ) of both clean Au(111) and SAM/Au(111) were measured using low photon energy ($h\upsilon = 60$ eV) and obtained using the equation $\phi = h\upsilon - W$, where W is the spectrum width (the energy difference between the substrate Fermi level and the low kinetic energy cutoff).[1] In order to resolve the low kinetic energy electrons, a -5 V sample bias was applied during measurements to compensate for the contact potential between the sample and the analyzer. The work function of the electron analyzer was measured to be 4.3 ± 0.05 eV.

Preparation of Self-Assembled Monolayers on Au(111). Synthesis details of 1-(*p*-thiophenyl)-4-phenylbenzene (BBB), 4-(*p*-thiophenyl)-2,2′,5,5′-tetramethoxy-biphenyl (BOO), 1-(*p*-thiophenyl)-4-(2′,5′-dimethoxyphenyl)-tetrafluorobenzene (BFO), and 4-pentafluorophenyl-1-(*p*-thiophenyl)-2,5-dimethoxybenzene (BOF) molecules will be reported elsewhere.[14] Monolayers of BBB, BOO, BFO, and BOF molecules were formed by spontaneous adsorption of their thioacetate forms [1-(*p*-acetylthiophenyl)-4-phenylbenzene for BBB, 4-(*p*-acetylthiophenyl)-2,2′,5,5′-tetramethoxy-biphenyl for BOO, 1-(*p*-acetylthiophenyl)-4-(2′,5′-dimethoxyphenyl)-tetrafluorobenzene for BFO, and 1-(*p*-acetylthiophenyl)-4-pentafluorophenyl-2,5-dimethoxybenzene for BOF] on Au(111)/mica substrates (SPI, U.S.A.). In all cases the Au(111)/mica samples were immersed in 3 mL of 1×10^{-4} M solutions in a N_2 environment for 48 h, using tetrahydrofuran (THF) as the solvent and 10 μL of 25% ammonia solution as the deprotection reagent to remove the acetyl protection groups.[15] After growth, the samples were thoroughly rinsed using THF and immediately transferred into an ultrahigh-vacuum (UHV) chamber (SINS beamline end station) with a base pressure of 5.0×10^{-11} torr.

Growth of CuPc on Au(111) and SAM/Au(111). Copper-(II) phthalocyanine (CuPc, Sigma-Aldrich, sublimation grade) molecules were evaporated in situ from a commercial low-temperature Knudsen cell (MBE Komponenten, Germany) onto the Au(111) and SAM/Au(111) substrates at room temperature in the main UHV chamber (base pressure of 5.0×10^{-11} torr) with a deposition rate of about 0.25 nm/min.[16] Before deposition, the CuPc was thoroughly degassed at 280 °C in UHV condition overnight. During deposition, the pressure was maintained below

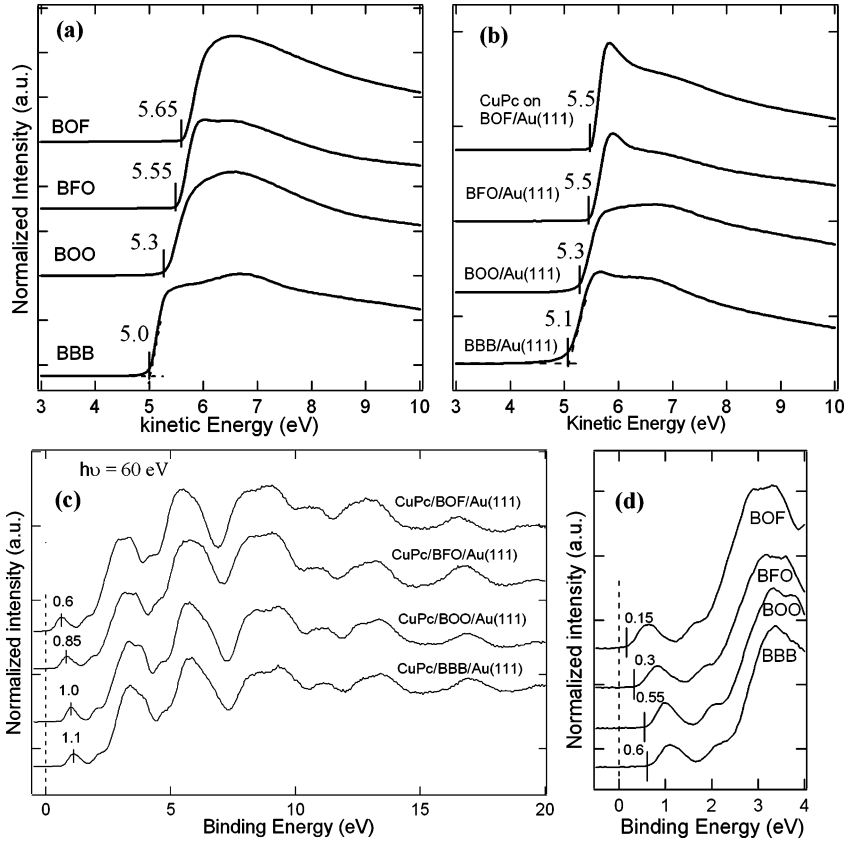

Figure 2. Synchrotron PES spectra at the low kinetic energy part for (a) clean SAMs/Au(111) samples (at a sample bias of -5 V) and (b) after deposition of 5 nm of CuPc. PES spectra for (c) the 5 nm CuPc/SAMs/Au(111) samples [relative to the E_F of Au(111)] and (d) near the E_F region of the spectra from part c. All spectra are measured with a photon energy of 60 eV.

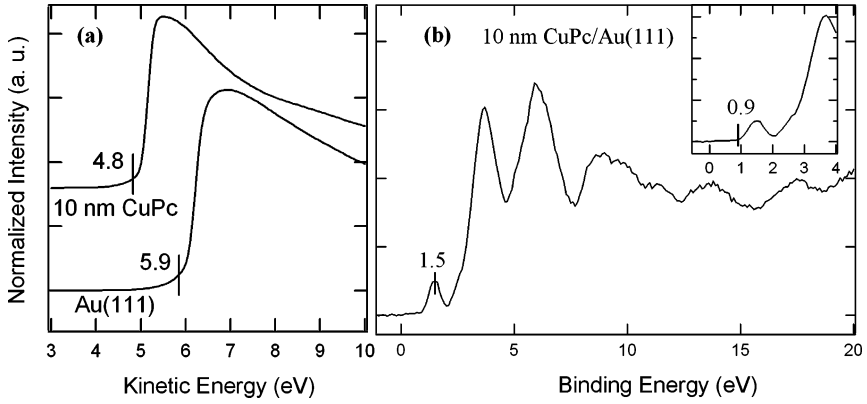

Figure 3. (a) Synchrotron PES spectra at the low kinetic energy part for clean Au(111) and 10 nm CuPc/Au(111). (b) PES spectra for the 10 nm CuPc/Au(111) samples [relative to the E_F of Au(111)] and near the E_F region of the spectrum (inset). All spectra were measured with a photon energy of 60 eV.

1.0×10^{-9} torr. The thickness of the CuPc layers on SAM/Au(111) was estimated by monitoring the attenuation in intensity of the Au $4f_{7/2}$ peak before and after deposition.[17] The Au(111) sample was cleaned through sputtering−annealing cycles to 450 °C.

Results and Discussion

Figure 2a shows the PES spectra at the low kinetic energy part for SAM/Au(111) samples. The vacuum levels (E_{vac}) of SAM/Au(111) with a −5 V sample bias were measured by linear extrapolation of the low kinetic energy onset (secondary electron cutoff) of PES spectra. The work functions (ϕ_{SAMs}) of SAM/Au(111) were determined to be 4.30 ± 0.05 eV for BBB/Au(111), 4.60 ± 0.05 eV for BOO/Au(111), 4.85 ± 0.05 eV for BFO/Au(111), and 4.95 ± 0.05 eV for BOF/Au(111). As compared to clean Au(111) with a work function (ϕ_{Au}) of 5.20 ± 0.05 eV as shown in Figure 3a, significant changes to the work functions upon the formation of SAMs on Au(111) were clearly observed. These changes can be attributed to the formation of an interface dipole (ID_1, $ID_1 = \phi_{SAMs} - \phi_{Au}$) on Au(111) by the functionalized SAMs, which is mainly determined by the intrinsic dipole moments of the different functionalized aromatic thiol molecules, as well as the surface area density of the thiol molecules and tilt angles of molecular axis with respect to the surface normal.[18a]

CuPc molecules were evaporated onto SAM/Au(111) in order to evaluate the effectiveness of tuning the hole injection barrier (Δ_h) using these functionalized SAMs. Figure 2b shows the PES spectra at the low kinetic energy part for SAM/Au(111) after deposition of 5 nm CuPc. The work functions (ϕ_{CuPc}) of 5 nm CuPc/SAM/Au(111) were measured and are summarized in Table 1. The interface dipole (ID_2) at the CuPc/SAMs is defined as $ID_2 = \phi_{CuPc} - \phi_{SAMs}$ and is also summarized in Table 1. The work functions of SAM/Au(111) are nearly constant after deposition of 5 nm of CuPc, indicating that there is no apparent interface dipole formation at the CuPc/SAMs interface. In contrast, a significant reduction of work function of about 1.1 ± 0.05 eV or an interface dipole of −1.1 eV was observed upon the deposition of 10 nm of CuPc on Au(111) (Figure 3a), which is mainly attributed to a lateral displacement of electronic charge by exchange repulsion upon adsorption of molecule layers on Au(111).[1−3,18] As previously reported, the vacuum level is nearly aligned at the organic/organic interface if no charge transfer occurs.[1,4c,19] Figure 4 shows the PES spectra at the low kinetic energy part for BBB/Au(111) and BOO/Au(111) with different CuPc coverages, showing that the vacuum level is almost aligned at the CuPc/SAM interfaces. The results also indicate that there is no charge-transfer complex formed at the CuPc/SAM interfaces. Such near vacuum level alignment upon the adsorption of CuPc on SAMs facilitates the effective tuning of Δ_h using these functionalized SAMs.

TABLE 1: Summary of Sample Parameters: Work Functions for Au(111) (ϕ_{Au}), SAMs/Au(111) (ϕ_{SAMs}), and Samples after Deposition of CuPc (ϕ_{CuPc}), Interface Dipole (ID_1) at the SAMs/Au(111) Interface, Interface Dipole (ID_2) at the CuPc/SAMs and CuPc/Au(111) Interfaces, and Hole Injection Barriers (Δ_h) between CuPc and the Au(111) Fermi Level[a]

	$\phi_{Au,SAMs}$ (eV)	ID_1 (eV)	ϕ_{CuPC} (eV)	ID_2 (eV)	Δ_h (eV)
Au(111)	5.20		4.10	−1.10	0.90
BBB	4.30	−0.90	4.40	0.10	0.60
BOO	4.60	−0.60	4.60	0	0.55
BFO	4.85	−0.35	4.80	−0.05	0.30
BOF	4.95	−0.25	4.80	−0.15	0.15

[a] The error bar is ± 0.05 eV.

Figure 2c shows the PES spectra for 5 nm CuPc/SAM/Au(111) at the low binding energy part, which agree well with previously published PES spectra of CuPc on metal surfaces.[2] In order to avoid the photohole screening effect on the determination of the binding energy of the CuPc HOMO peak commonly observed for ultrathin organic film on metal surfaces,[2e] a relatively thick CuPc film of 5 nm on SAMs/Au(111) was used in our experiments. As shown in Figure 2c, the HOMO peak maxima of the CuPc layers are obviously different after 5 nm of CuPc was deposited on different SAM/Au(111) substrates, i.e., the HOMO peak is centered at 1.1 ± 0.05 eV (binding energy scale) for 5 nm of CuPc on BBB/Au(111), 1.0 ± 0.05 eV for CuPc/BOO/Au(111), 0.85 ± 0.05 eV for CuPc/BFO/Au(111), and 0.6 ± 0.05 eV for CuPc/BOF/Au(111). Figure 2d shows the closeup of the region near the Fermi level in Figure 2c. The hole injection barrier (Δ_h) of CuPc can be measured from the energy difference between the substrate Fermi level and the HOMO leading edge (linear extrapolation of the low binding energy onset).[1−4] A Δ_h of as small as 0.15 ± 0.05 eV was observed for CuPc/BOF/Au(111). The Δ_h of CuPc deposited on different SAMs/Au(111) were measured and are summarized in Table 1. In comparison to the Δ_h of 0.9 ± 0.05 eV for CuPc on Au(111) shown in Figure 3b, a significant reduction of Δ_h by as much as 0.75 eV was achieved after modifying the Au(111) with BOF SAMs. The schematic energy level diagrams of CuPc on Au(111) and SAMs/Au(111) are displayed in Figure 5. The results clearly demonstrate the effective tuning of Δ_h using these functionalized SAMs.

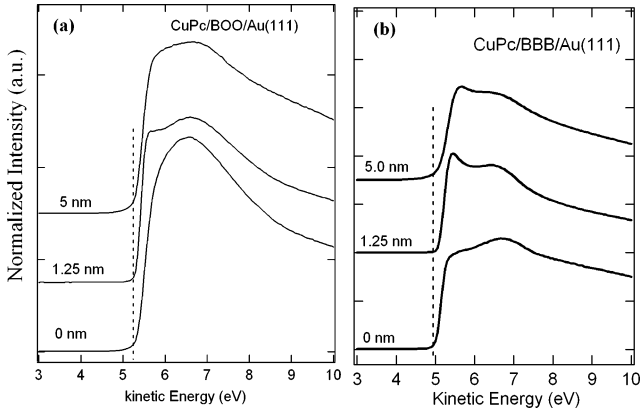

Figure 4. Synchrotron PES spectra at the low kinetic energy part for (a) CuPc/BOO/Au(111) and (b) CuPc/BBB/Au(111) with a CuPc coverage at 1.25 and 5.0 nm.

The molecular orientations of CuPc on SAMs/Au(111) were probed by NEXAFS, which can be used to monitor the resonance from the core level of a specific atomic species of a molecule (for example, the K-shell of carbon or nitrogen atoms in a molecule) to its unoccupied molecular orbitals (π^* and σ^* orbitals).[13] In principle, the resonance to the unoccupied π^* or σ^* orbital is strong when the electronic field vector **E** of the incident linear polarized synchrotron light has a large projection along the direction of the π^* or σ^* orbital, and it vanishes when **E** is perpendicular to the π^* or σ^* orbital.[13] For the disklike CuPc molecules, the σ^* and π^* orbitals are directed essentially in-plane and out-of-plane, respectively. Therefore, the angular-dependent NEXAFS can be used to probe the molecular orientation of CuPc on SAMs/Au(111). Figure 6 shows the nitrogen K-edge NEXAFS spectra of 5 nm CuPc/SAMs/Au(111) as a function of the synchrotron light incidence angle θ. The first three sharp absorption peaks are assigned to excitations from the N 1s core level to individual π^* states, and the broad absorption peaks at the higher photon energy part are transitions to the σ^* states.[20,21] The maximum intensity of the π^* resonances for all the CuPc/SAMs/Au(111) is observed at normal incidence ($\theta = 90°$), whereas the maximum intensity of the σ^* resonances is observed at grazing incidence ($\theta = 20°$). This indicates that the CuPc molecules on SAMs/Au(111) are in a standing up configuration with the molecular plane nearly normal to the Au(111) surface. The intensity I of the π_1^* resonance is related to the tilt angle α of the CuPc molecular plane with respect to the Au(111) surface plane and the synchrotron light incidence angle θ by[13]

$$I(\theta) \propto 1 + \frac{1}{2}(3\cos^2\theta - 1)(3\cos^2\alpha - 1)$$

Using the intensity ratio $R(\pi_1^*) = I(90°)/I(20°)$, we calculate the tilt angle α for 5 nm CuPc/BBB/Au(111) to be $58° \pm 5°$, $\alpha = 76° \pm 5°$ for CuPc/BFO/Au(111), $\alpha = 73° \pm 5°$ for CuPc/

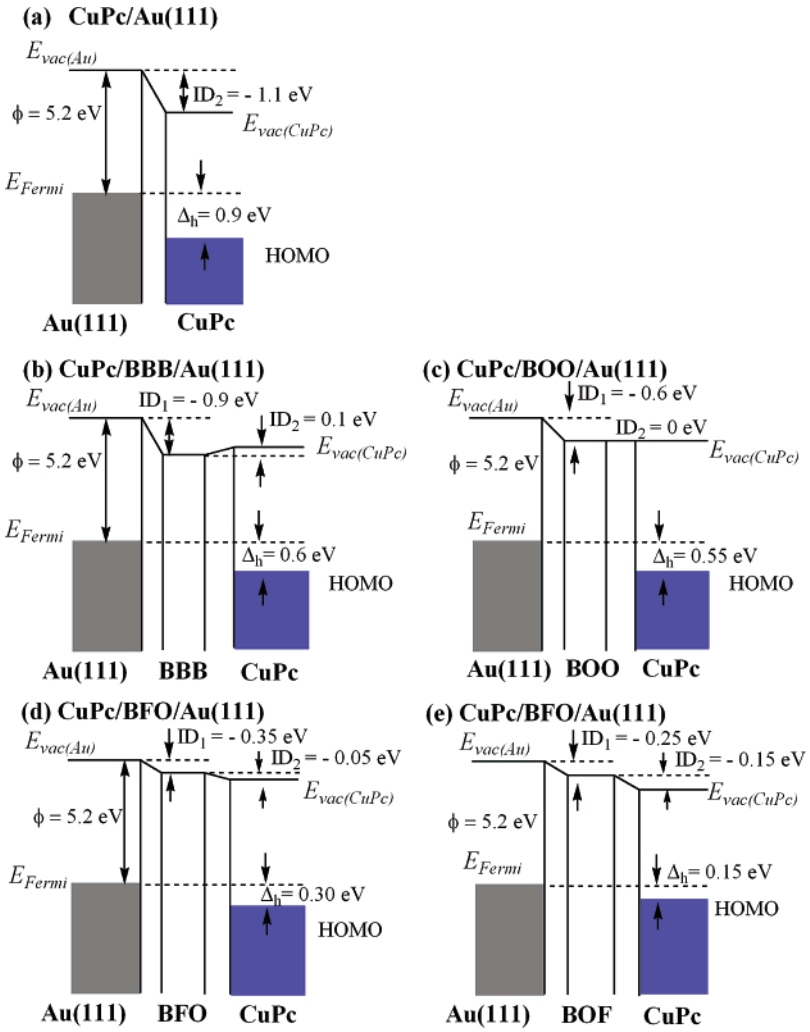

Figure 5. Schematic energy level diagrams of CuPc on (a) Au(111), (b) BBB/Au(111), (c) BOO/Au(111), (d) BFO/Au(111), and (e) BOF/Au(111).

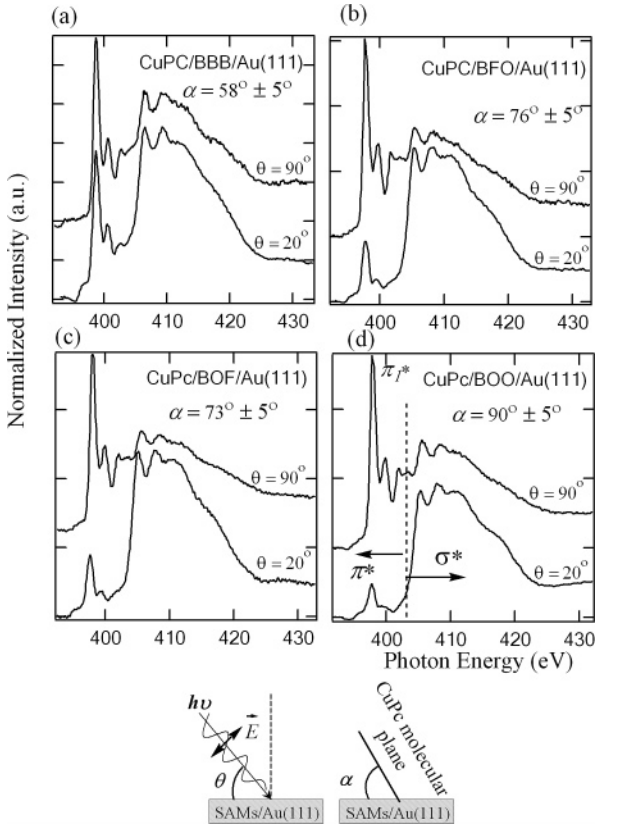

Figure 6. Nitrogen K-edge NEXAFS spectra for the 5 nm CuPc on (a) BBB/Au(111), (b) BFO/Au(111), (c) BOF/Au(111), and (d) BOO/Au(111) as a function of the synchrotron light incident angle.

BOF/Au(111), and $\alpha = 90° \pm 5°$ for CuPc/BOO/Au(111). The orientation of CuPc on SAMs/Au(111) is obviously different from that of CuPc on Au(111). On Au(111), CuPc is in a lying down configuration with a tilt angle $\alpha = 20° \pm 5°$ due to the relative strong metal−molecule interaction at the CuPc/Au(111) interface.[16,20] In contrast, the interaction between CuPc and underlying SAMs is dominated by the weak van der Waals force, leading to a standing up configuration of CuPc on SAMs, as observed for pentacene on SAMs.[22] As shown in Figure 6, although there are some variations in the tilt angles of CuPc on different SAMs/Au(111), the CuPc on SAM/Au(111) are all generally in a standing up configuration. It has been reported that the organic molecules such as pentacene and CuPc adopt a near-vertical orientation on the underlying oxide substrate surfaces.[20,23] In a proposed OFET device using gold as the source and drain electrodes, SiO_2 as the gate insulator, and CuPc as the organic semiconductor, the upright orientation of CuPc on SAM-modified Au(111) allows the $\pi-\pi$ stacking direction of the CuPc molecules to remain parallel to the CuPc/SiO_2 interface from the source electrode through the gate insulator to the drain electrode, thereby facilitating the efficient hole transport in the conduction channel during device operation.

In conclusion, self-assembled functionalized aromatic thiols (oligophenylenes composed of building blocks of dimethoxy-substituted phenylenes, perfluoro-substituted phenylenes, and a terminal thiol group) adsorbed on Au(111) were used to tune the hole injection barrier (Δ_h) of copper(II) phthalocyanine (CuPc) on Au(111). The electronic structures at the CuPc/SAM/Au(111) interfaces were investigated by synchrotron-based high-resolution photoemission spectroscopy. A significant reduction of Δ_h by up to 0.75 eV was observed after deposition of 5 nm of CuPc on BOF/Au(111) as compared to that of CuPc/Au(111) ($\Delta_h = 0.9$ eV). A Δ_h value of as low as 0.15 eV was achieved for CuPc/BOF/Au(111). Our results also reveal near vacuum level alignment at the CuPc/SAM interface. The molecular orientations of CuPc on SAM/Au(111) were probed by NEXAFS, showing an upright configuration of CuPc on SAMs, facilitating their effective incorporation in OFET and other planar organic devices.

Acknowledgment. W. Chen acknowledges the support from National University of Singapore under the Grants R-144-000-107-112 and R-398-000-036-305. This work was partly performed at SSLS under NUS Core Support C380-003-003-001, A*STAR/MOE RP 3979908M, and A*STAR 12 105 0038 Grants.

References and Notes

(1) Ishii, H.; Sugiyama, K.; Ito, E.; Seki, K. *Adv. Mater.* **1999**, *11*, 605.

(2) (a) Knupfer, M.; Peisert, H. *Phys. Status Solidi A* **2004**, *201*, 1055. (b) Peisert, H.; Knupfer, M.; Zhang, F.; Petr, A.; Dunsh, L.; Fink, J. *Appl. Phys. Lett.* **2003**, *83*, 3930. (c) Peisert, H.; Knupfer, M.; Schwieger, T.; Fuentes, G. G.; Olligs, D.; Fink, J.; Schmidt, T. *J. Appl. Phys.* **2003**, *93*, 9683. (d) Peisert, H.; Knupfer, M.; Fink, J. *Appl. Phys. Lett.* **2002**, *81*, 2400. (e) Peisert, H.; Knupfer, M.; Schwieger, T.; Auerhammer, J. M.; Golden, M. S.; Fink, J. *J. Appl. Phys.* **2002**, *91*, 4872.

(3) (a) Koch, N.; Duhm, S.; Rabe, J. P.; Vollmer, A.; Johnson, R. L. *Phys. Rev. Lett.* **2005**, *95*, 237601. (b) Koch, N.; Duhm, S.; Rabe, J. P.; Rentenberger, S.; Johnson, R. L.; Klankermayer, J.; Schreiber, F. *Appl. Phys. Lett.* **2005**, *87*, 101905. (c) Koch, N.; Elschner, A.; Rabe, J. P.; Johnson, R. L.; *Adv. Mater*. **2005**, *17*, 330. (d) Koch, N.; Elschner, A.; Schwartz, J.; Kahn, A. *Appl. Phys. Lett.* **2003**, *82*, 2281. (e) Koch, N.; Kahn, A.; Ghijsen, J.; Pireaux, J. J.; Schwartz, J.; Johnson, R. L. Elschner, A. *Appl. Phys. Lett.* **2003**, *82*, 70.

(4) (a) Vazquez, H.; Gao, W.; Flores, F.; Kahn, A. *Phys. Rev. B* **2005**, *71*, 041306. (b) Kera, S.; Yabuuchi, Y.; Yamane, H.; Setoyama, H.; Okudaira, K. K.; Kahn, A.; Ueno, N. *Phys. Rev. B* **2004**, *70*, 085304. (c) Kahn, A.; Koch, N.; Gao, W. Y. *J. Polym. Sci., Part B: Polym. Phys.* **2003**, *41*, 2529.

(5) (a) Bruner, E. L.; Koch, N.; Span, A. R.; Bernasek, S. L.; Kahn, A.; Schwartz, J. *J. Am. Chem. Soc.* **2002**, *124*, 3192. (b) Hanson, E. L.; Guo, J.; Koch, N.; Schwartz, J.; Bernasek, S. L. *J. Am. Chem. Soc.* **2005**, *127*, 10058. (c) Guo, J.; Koch, N.; Schwartz, J.; Bernasek, S. L. *J. Phys. Chem. B* **2005**, *109*, 3966. (d) McDowell, M.; Hill, I. G.; McDermott, J. E.; Bernasek, S. L. Schwartz, J. *Appl. Phys. Lett.* **2006**, *88*, 073505. (e) Yan, H.; Huang, Q.; Cui, J.; Veinot, J. G. C.; Kern, M. M.; Marks, T. J. *Adv. Mater.* **2003**, *15*, 835.

(6) (a) Khodabakhsh, S.; Sanderson, B. M.; Nelson, J.; Jones, T. S.; *Adv. Funct. Mater.* **2006**, *16*, 95. (b) Khodabakhsh, S.; Poplavskyy, D.; Heutz, S.; Nelson, J.; Bradley, D. D.; Murata, H.; Jones, T. S. *Adv. Funct. Mater.* **2004**, *14*, 1205.

(7) Tang, J. X.; Li, Y. Q.; Hung, L. S.; Lee, C. S. *Appl. Phys. Lett.* **2004**, *84*, 73.

(8) Osikowicz, W.; Crispin, X.; Tengstedt, C.; Lindell, L.; Kugler, T.; Salaneck, W. R. *Appl. Phys. Lett.* **2004**, *85*, 1616.

(9) (a) de Boer, B.; Hadipour, A.; Mandoc, M. M.; van Woudenbergh, T.; Bolm, P. W. M. *Adv. Mater*. **2005**, *17*, 621. (b) Campbell, I. H.; Kress, J. D.; Martin, R. L.; Smith, D. L.; Barashkov, N. N.; Ferraris, J. P. *Appl. Phys. Lett.* **1997**, *71*, 3528.

(10) Alloway, D. M.; Hofmann, M.; Smith, D. L.; Gruhn, N. E.; Graham, A. L.; Colorado, R.; Wysocki, V. H.; Lee, T. R.; Lee, P. A.; Armstrong, N. R. *J. Phys. Chem. B* **2003**, *107*, 11690.

(11) Zehner, R. W.; Parsons, B. F.; Hsung, R.; Sita, L. R. *Langmuir* **1999**, *15*, 1121.

(12) (a) Chen, W.; Xu, H.; Liu, L.; Gao, X. Y.; Qi, D. C.; Peng, G. W.; Tan, S. C.; Feng, Y. P.; Loh, K. P.; Wee, A. T. S. *Surf. Sci.* **2005**, *596*, 176. (b) Yu, X. J.; Wilhelmi, O.; Moser, H. O.; Vidyarai, S. V.; Gao, X. Y.; Wee, A. T. S.; Nyunt, T.; Qian, H.; Zheng, H. *J. Electron. Spectrosc. Relat. Phenom.* **2005**, *144−147*, 1031.

(13) Stöhr, J. *NEXAFS Spectroscopy*; Springer-Verlag: Berlin, New York, 1992.

(14) Huang, C.; Yang, J. S.; Chen, W.; Loh, K. P.; Wee, A. T. S.; Chen, Z. K. Manuscript in preparation.

(15) Chen, W.; Wang, L.; Huang, C.; Lin, T. T.; Gao, X. Y.; Loh, K. P.; Chen, Z. K.; Wee, A. T. S. *J. Am. Chem. Soc.* **2006**, *128*, 935.

(16) Chen, W.; Wang, L.; Qi, D.; Chen, S.; Wee, A. T. S. *Appl. Phys. Lett.* **2006**, *88*, 184102.

(17) (a) Schwieger, T.; Peisert, H.; Golden, M. S.; Knupfer, M.; Fink, J. *Phys. Rew. B* **2002**, *66*, 155207. (b) Seah, M. P.; Dench, W. A. *Surf. Interface Anal.* **1979**, *1*, 2.

(18) (a) de Renzi, V.; Rousseau, R.; Marchetto, D.; Biagi, R.; Scandolo, S.; del Pennino, U. *Phys. Rev. Lett.* **2005**, *95*, 046804. (b) Bagus, P. S.; Staemmler, V.; Wöll, C. *Phys. Rev. Lett.* **2002**, *89*, 096104. (c) da Silva, J. L. F.; Stampfl, C. Scheffler, M. *Phys. Rev. Lett.* **2003**, *90*, 066104. (d) Witte, G.; Lukas, S.; Bagus, P. S.; Wöll, C. *Appl. Phys. Lett.* **2005**, *87*, 263502. (e) Ahn, H.; Zharnikov, M.; Whitten, J. E. *Chem. Phys. Lett.* **2006**, *428*, 283.

(19) Tang, J. X.; Lau, K. M.; Lee, C. S.; Lee, S. T. *Appl. Phys. Lett.* **2006**, *88*, 232103.

(20) Peisert, H.; Schwieger, T.; Auerhammer, J. M.; Knupfer, M.; Golden, M. S.; Fink, J. *J. Appl. Phys.* **2001**, *90*, 466.

(21) de Jong, M. P.; Friedlein, R.; Sorensen, S. L.; Öhrwall, G.; Osikowicz, W.; Tengsted, C.; Jönsson, S. K. M.; Fahlman, M.; Salaneck, W. R. *Phys. Rev. B* **2005**, *72*, 035448.

(22) Hu, W. S.; Tao, Y. T.; Hsu, Y. J.; Wei, D. H.; Wu, Y. S. *Langmuir* **2005**, *21*, 2260.

(23) Fritz, S. E.; Martin, S. M.; Frisbie, C. D.; Ward, M. D.; Toney, M. F. *J. Am. Chem. Soc.* **2004**, *126*, 4084.